ISSN No:-2456-2165 https://doi.org/10.38124/ijisrt/25mar287

Groundwater Potential Zones and Storage Capacity of Aquifer in Parsa District, Nepal

Subrat Adhikari[1]; Mahesh Prasad Bhattarai[2]; Pratap Singh Tater[3]

[1;2]Tribhuvan University Institute of Engineering, Lalitpur, Nepal
[3]Consultant Hydrogeologist, Nepal

Publication Date: 2025/03/22

Abstract: Dependency on groundwater in southern flatlands (Terai) of Nepal is high because of its reliability. Random excessive pumping may cause depletion of groundwater. Combination of Multi-Criteria Decision Analysis (MCDA) technique like Analytical Hierarchy Process (AHP) with Geographical Information System (GIS) tool aids in identifying the ground- water potential zones in different environmental settings. The study was conducted in Parsa district and provides a basis for the availability of groundwater. The objective of this study is to map the groundwater potential zones and calculate the storage capacity of an aquifer up to 50 m depth. A new theme of groundwater potential zones was obtained from seven different themes by using weighted overlay tool. Potential groundwater storage capacity of shallow aquifer was obtained by the help of thickness of aquifer and porosity of permeable layer. Permeable layer depths were interpolated using ordinary Kriging. An area of about 14.67 km^2, 213.26 km^2, 840.90 km^2 and 284.18 km^2 of study realm exhibited poor, moderate, good, and very good groundwater potential zone respectively. Approximately 70 % of total study area has a permeable layer between 9.21 to 11.79 m within depth of 50 m of shallow aquifer as obtained by ordinary Kriging method. A total of 5072.84 million cubic meters of water can be stored in the permeable layer of shallow aquifer up to 50 m depth. The chances of establishing groundwater potential storage zone were better in regions that had non-residential areas, flatlands, low surface drainage density, high rainfall and fertile soil based on weighted overlay.

Keywords: *Groundwater Potential Zones, GIS, Potential Storage, AHP, Parsa.*

How to Cite: Subrat Adhikari; Mahesh Prasad Bhattarai; Pratap Singh Tater (2025). Groundwater Potential Zones and Storage Capacity of Aquifer in Parsa District, Nepal. *International Journal of Innovative Science and Research Technology*, 10(3), 648-667. https://doi.org/10.38124/ijisrt/25mar287

I. INTRODUCTION

From subtropical to semi-arid climatic conditions, groundwater is used extensively for drinking and irrigation purposes [1]. Dependency on groundwater to meet domestic and industrial water demand in southern flatlands (Terai) of Nepal is high whereas for irrigation groundwater is the reliable source throughout the year [2]. More than 2 billion people around the world use groundwater as the primary source of water and approximately 50 % of the total water used for irrigation is contributed by groundwater [3]. Every year groundwater withdrawals total 750–800 km^3 around the world and unrestrained groundwater exhaustion affects major regions of North Africa, the Middle East, South and Central Asia, North China, North America, and Australia [4]. Globally, the share of groundwater used for consumptive purpose is 43 % [5].

In the Indian context, 90 % people in rural areas and 30 % of the population in cities depend on groundwater to fulfil their daily basic requirements [6]. In the last half century, abstraction of groundwater has increased from about 10–20 km^3/year to nearly 260 km^3/year in the Indian subcontinent [7]. Nearly 30 % of the world population is affected by groundwater stress of at least 50 % [8]. The significance of groundwater resources has increased in the present due to the threat imposed by climate change on water supplies [9]. Groundwater is spatially distributed, and it provides natural storage of water by protecting from surface evaporation especially in areas having high evaporation and limited rainfall [10]. The covering layer capping the aquifer as well as the aquifer matrix plays key role in the occurrence of groundwater [11].

In the context of Nepal, the plain flatlands of Terai cover 17 % of the total area while the rest of the area is covered by mountainous and hilly region. Availability of groundwater is sufficient in the Terai region [12], but the ever-growing population has increased the demands for groundwater. The groundwater demand has increased primarily because of the agricultural activities as the soil are high yielding in majority areas of the Terai belt. The annual population growth rate of Terai region is 1.56 % according to the annex of preliminary report of

ISSN No:-2456-2165 https://doi.org/10.38124/ijisrt/25mar287

census 2021 [13] which is the highest when compared with the three geographical belts of Nepal. This study that was carried out in Parsa district will provide a basis for the availability of groundwater in that zone.

Geographical Information System and remote sensing cover large and inaccessible areas within short time with the availability of spatial and temporal data [14]. Remote sensing and GIS technique has become popular means among the researchers in last decade for the assessment of groundwater potential zone worldwide [1]. Multi-Criteria Decision Analysis (MCDA) technique such as Analytical Hierarchy Process (AHP) can be coupled with remote sensing data and GIS tools to identify the groundwater potential zones [15] in different geo-environmental settings, which implies the capability and reliability of the techniques for groundwater management [16]. GIS process and field studies work hand in hands, in which the course of action of the former helps in amalgamation and investigation of huge amount of data, whereas the latter contributes by validating the results [17]. GIS techniques can be utilized for assessment of groundwater aquifers, water sustainability and decision making [18].

AHP and cost-benefit analysis are namely some of the methods that are being used for the MCDA [3]. In recent times, globally, the researchers have been using AHP with GIS in various environmental suitability studies [19]. The latest studies shows that the integration of GIS with MCDA techniques such as AHP developed by Saaty (1980) [20] gave good results [21, 22] in identifying potential groundwater zones with the aid of which groundwater potential map can be prepared [9, 23]. Spatial calculation of the physical capacity of the topography to yield sufficient groundwater for a given use is described as groundwater potential map [24]. Groundwater potential zones can be identified successfully by proper assignment of weights and by taking adequate number of thematic layers into account [25]. GIS is used for determining groundwater potential zones to minimize costs and reinforce other survey findings [9, 26]. Combination of remote sensing, GIS, and AHP is one of the most common, dependable, and economical approaches for assessing groundwater identification, recharge, and storage [27].

Porosity and other hydraulic parameters across an area assist in describing the groundwater flow system [28]. Range of values of porosity as per Freeze and Cherry, 1979 [29] is presented in Table 1. Porosity is the ratio of volume of voids to the total volume and can be calculated using Equation 1:

$$\Phi = V_V/V_T \quad (1)$$

Where ϕ is the porosity of the medium, V_V is the volume of voids and V_T is the total volume.

Table 1 Range of values of Porosity

Unconsolidated Deposits	Porosity, n (%)
Gravel	25-40
Sand	25-50
Silt	35-50
Clay	40-70

The goal of this study is to map the potential groundwater extraction zone and to calculate the potential water storage capacity in Parsa district. The groundwater potential map generated from this study may also be helpful to practitioners who want to install hand pumps in public places or extract groundwater for drinking, industrial or irrigation purposes in the district.

II. STUDY AREA

Parsa district that covers an area of 1,353 km^2 was selected as the study area (Figure 1). Parsa district lies between 84° 29’ 10” E to 84° 58’ 28” E and 26° 59’ 04” N to 27° 27’ 46” N. Majority of the study area lies in lower tropical climate zone. The elevation varies between 81 to 83 meters above sea level (masl) with an average elevation of 235 masl. Most of the rivers flow from north to south direction in the study area with the major rivers being Tilawe and Shikta [30].

ISSN No:-2456-2165 https://doi.org/10.38124/ijisrt/25mar287

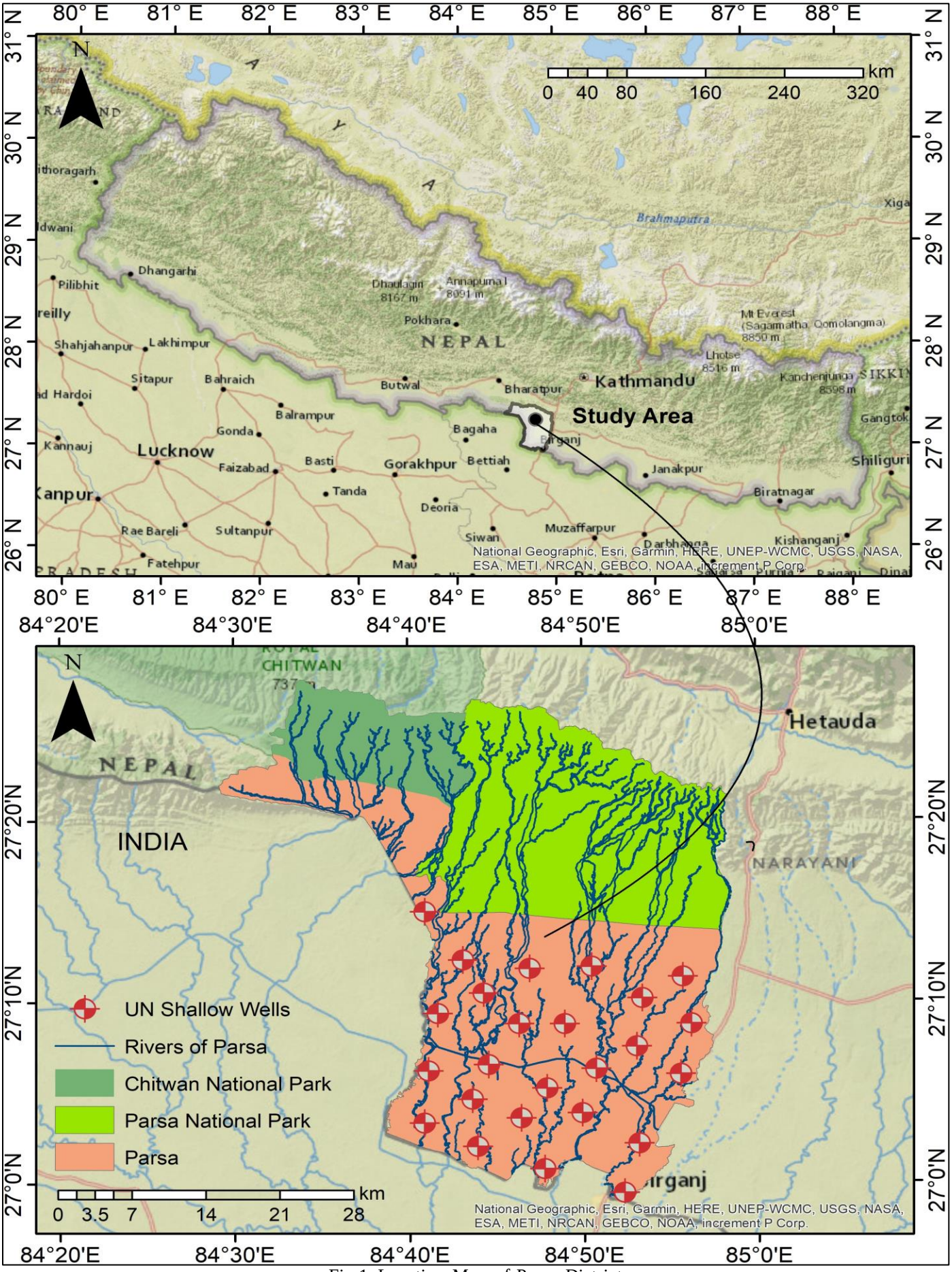

Fig 1 Location Map of Parsa District

ISSN No:-2456-2165 https://doi.org/10.38124/ijisrt/25mar287

Forests cover 762.56 km^2 of the total area [31]. Majority of the forest areas in Parsa are occupied by Parsa National Park and Chitwan National Park which primarily lies in the northern part of the district. Thick clay deposits lie right below the ground level in the southern half of the district due to which direct recharge by infiltrated rainfall becomes less effective. So, the recharge of the top 50 m below ground level takes place by lateral flow from northern parts of the district where National Parks are located along with minimal direct recharge [30].

Northern and southern parts of Parsa district are more permeable than central part of the district. Similarly, the value of transmissivity rises if we move towards the north, ranging from 500 to 2600 m^2/d. Towards the central part, transmissivity is below 100 m^2/d while the southern part lies in between 100 to 300 m^2/d. Water level in the district is between 2 to 5 meters below ground level (mbgl) in May except for Nirmal Basti area where the water level is around 15 to 17 mbgl. Whereas the water level varies between 0.5 to 3 mbgl in September. In terms of water level, the southern part is shallower than the northern part. General direction of groundwater is from north to south and the average gradient of flow is about 0.002 [30].

Geologically, the highland Siwalik region lies in the northern and north-western part of the district while the Gangetic plain is spread across the central and southern part of the district. Predominantly, the fan deposits near the Siwalik hills and mountains are the source of recharge to shallow aquifers [30]. The annual rainfall in 2021 was recorded as 1950.82 mm by Birgunj station in Parsa district [32]. The average evapotranspiration from 2001 to 2021 of the study area is 923.76 mm [33]. From June to September, the average monthly evapotranspiration is exceeded by average monthly rainfall [30]. According to the measurements made by Simara airport station from 1990 to 2021, the maximum and minimum annual average temperatures of Parsa district are 30.51℃ and 18.27℃ respectively [32].

III. METHODOLOGY

Slope and lineament density was calculated using 100 m resolution Digital Elevation Model (DEM) which was retrieved in 2019 and made available to the public through Department of Survey (DoS) [34]. Data of rivers of Parsa district was extracted from Rivers of Nepal digital data in GIS which was also retrieved in 2019 from DoS [35]. Land cover data of 2021 was collected from ESRI [31] via Sentinel-2 10 m Land use/ land cover time series. In the same way, soil and geology data was collected from database of FAO [36] and ICIMOD [37] respectively. Precipitation data was collected from Department of Hydrology and Meteorology (DHM) [32] of Simara, Birgunj, Parwanipur and Thori climatic stations starting from the year 1990 to 2021.

Maps related to groundwater potential zones and permeable layer map are generated using ArcGIS 10.2.2. The standard error of Ordinary Kriging interpolation method along with semi variogram modelling was calculated using Geostatistical tool within GIS environments.

Based on slope, land use, soil, precipitation, geology, lineament density and surface drainage density, groundwater potential zones were identified using GIS and AHP. For preparation of precipitation map of Parsa district, precipitation values of all four stations were used. Using AHP, appropriate weights were assigned to parameters based on review of literature and opinion of experts followed by the calculation of normalized weights which were calculated through pairwise comparison between thematic layers of study area. Land cover was assigned the highest weight of 7 while on the contrary soil type was assigned the lowest weight of 2.5 when performing pairwise comparison between thematic layers. Land cover was assigned the highest weight because it was the most variable theme in the study area. On the other hand, soil type was assigned the lowest weight because the study area had only two soil types. Eventually, values of consistency ratio and consistency index were calculated. Then, raster themes having several sub-classes were overlaid in ArcGIS with their normalized weights along with the assigned ranks for each sub-class using ′Weighted Overlay′ tool. The calculation as mentioned in Equation 4 was carried out and groundwater potential was estimated. Values of 4, 4-5, 5-6 and 6-7 were obtained which were labelled as poor, moderate, good and very good respectively to mark them as groundwater potential classes. Hence, a new theme of groundwater potential zone was prepared. The new prepared map of groundwater potential zone was categorized into several classes such as very good, good, moderate, and poor. Then, based on the location of the wells [30], the new prepared map of groundwater potential zone was validated. The section of the wells was based on hydrogeological survey of Parsa district, which was conducted in 1990 [30].

After creation of new thematic map, raster data was converted to vector data by the help of ′Raster to Polygon′ conversion tool. Then within attribute table of new polygon map, area in square kilometres of the polygons was calculated using ′Calculate Geometry′ option. Then the data of entire attribute table was exported to MS Excel where areas of different potential zones were calculated using ′Sum′ function.

Water storage potential of the permeable layer up to depth of 50 m was calculated by determining the permeable depth at different well locations based on the UNDP and HMG, 1990 [30]. Though the depth of numerous wells in Parsa district could have been more than 50 m, but the depth for each well was taken only up to 50 m in this study to maintain consistency and to increase the number of selected wells. Permeable depth was interpolated using ordinary Kriging and the range of

ISSN No:-2456-2165 https://doi.org/10.38124/ijisrt/25mar287

permeable depth along with the coverage area was obtained. This area when multiplied with permeable depth and porosity of material gave the water storage potential capacity in MCM of shallow aquifer up to depth 50 m.

IV. RESULTS AND DISCUSSION

A. Parameters Affecting Groundwater Potential

In this study, seven factors namely land use/land cover (LC), slope (S), geology (G), drainage density (DD), precipitation (P), lineament density (LD) and soil type (ST) are considered for identifying groundwater potential zones.

➢ *Land use/Land cover*

Land use/Land cover includes soil deposits, vegetation cover and distribution of residential areas [38]. Surface water flow to rivers increases with the change in land-use along with urbanization [39]. The connection between groundwater and land-use is very close; also, there is lack of understanding of subsurface environment by most people, especially policy makers, engineers and managers without a geological training as aquifers outcrop over a large area and groundwater cannot be seen [40]. Changing recharge conditions and water demand depends on LULC features which affect groundwater resources [9]. Favourable conditions for recharge are created with high-intensity rainfall along with a poor vegetation cover on a permeable soil or fractured porous bedrock near the surface [41].

Generally, areas with water bodies, built up area and barren land have low groundwater potential. Soil beneath water bodies is less likely to recharge due to low infiltration. In built up areas, recharge is significantly low as most of the surface is concrete and large amount of precipitation is lost in the form of runoff. Due to the presence of unfertile and hard soils in barren lands, the groundwater potential in those lands is minimal. Ground water potential is favoured by the presence of forest, agricultural land, grassland and shrubland. Moreover, the role of vegetation becomes more crucial as it helps in the prevention of direct evaporation of water from the soil [38].

In the case of land use/land cover of 2021, data was obtained from ESRI [31] via Sentinel-2 10 m LULC time series which was used in the GIS environment. Land use map of Parsa district is presented in Figure 2.

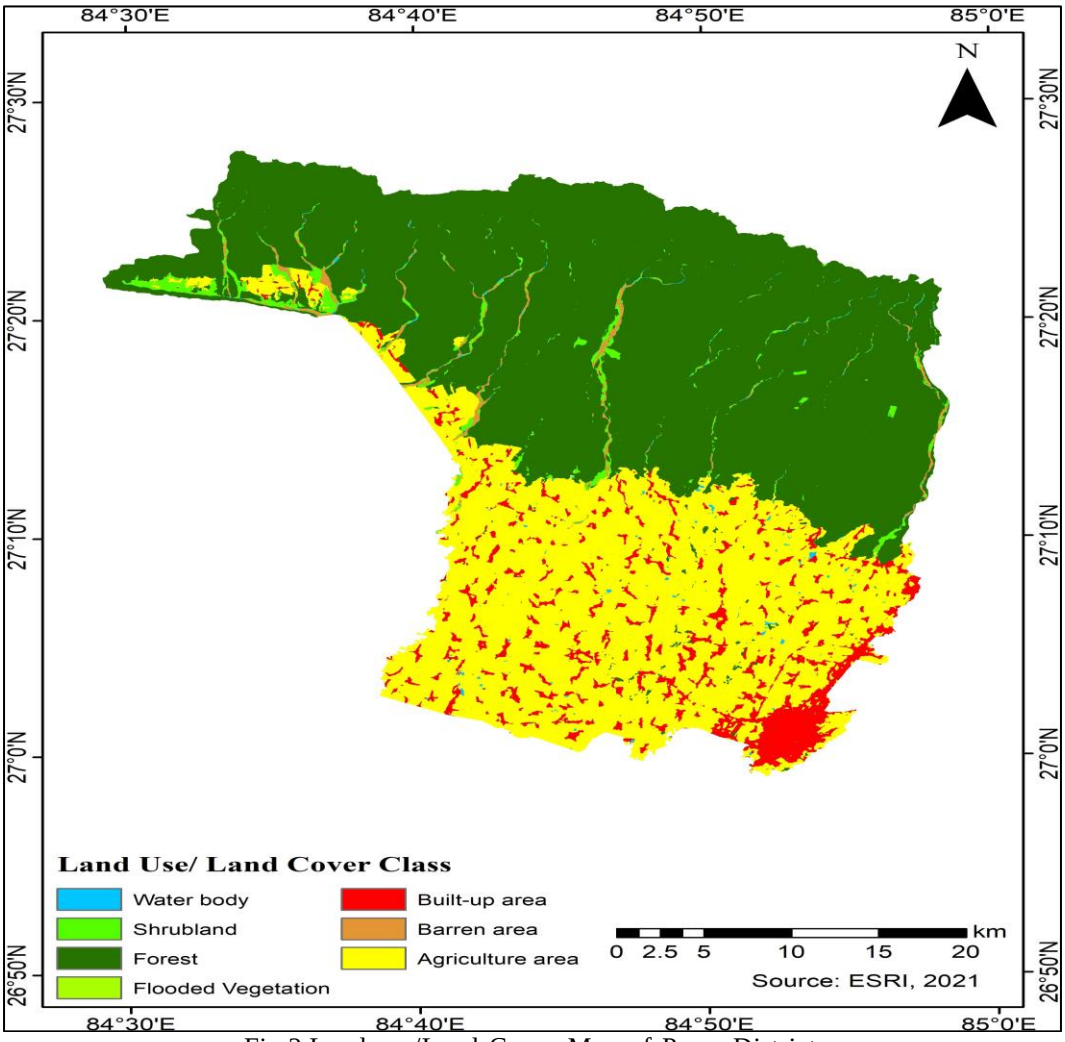

Fig 2 Land use/Land Cover Map of Parsa District

ISSN No:-2456-2165 https://doi.org/10.38124/ijisrt/25mar287

Calculation revealed that as of 2021 Parsa district had 56.36 % (762.56 km^2) forest, 34.99 % (473.41 km^2) agriculture area, 0.89 % (11.99 km^2) barren area, 5.69 % (76.92 km^2) built-up area, 0.35 % (4.75 km^2) water body, 1.73 % (23.37 km^2) shrubland and insignificant flooded vegetation area.

➢ *Slope*

Slope is one of the significant factors that affect groundwater potential. Slope defines the type of surface topography and shallow groundwater levels essentially follow it [7]. The infiltration of rainfall is directly influenced by slope gradient/steepness which makes it an important indicator for the suitability for groundwater prospect in a particular region [42]. In most cases, groundwater potential increases as slope value decreases [43, 44, 9]. Surface runoff is slow in areas with mild or gentle slope that allows more time for rainwater to percolate, whereas time for rainwater to percolate in areas with steep slope is less due to which surface runoff is high and hence less infiltration into the surface along with limited time to recharge the saturated zone [45, 42, 38].

Slope values are expressed in degree rise and lies in between 0 to 90 degrees. Areas with less degree rise in slope indicate flatlands. Higher slope values are observed in the highlands area while the midlands that are sandwiched between highlands and flat lowlands may have intermediate value of degree rise in slope. The slope of Parsa district calculated in GIS by the help of data obtained from Digital Elevation Model (DEM) which is made available to the public by Department of Survey. The above-mentioned calculation reveals that the slope of Parsa district lies in the range of 0.00° to 33.11° provided in Figure 3 with 70.53 % (954.31 km^2) of total land lying in the range of 0.00° to 2.08°.

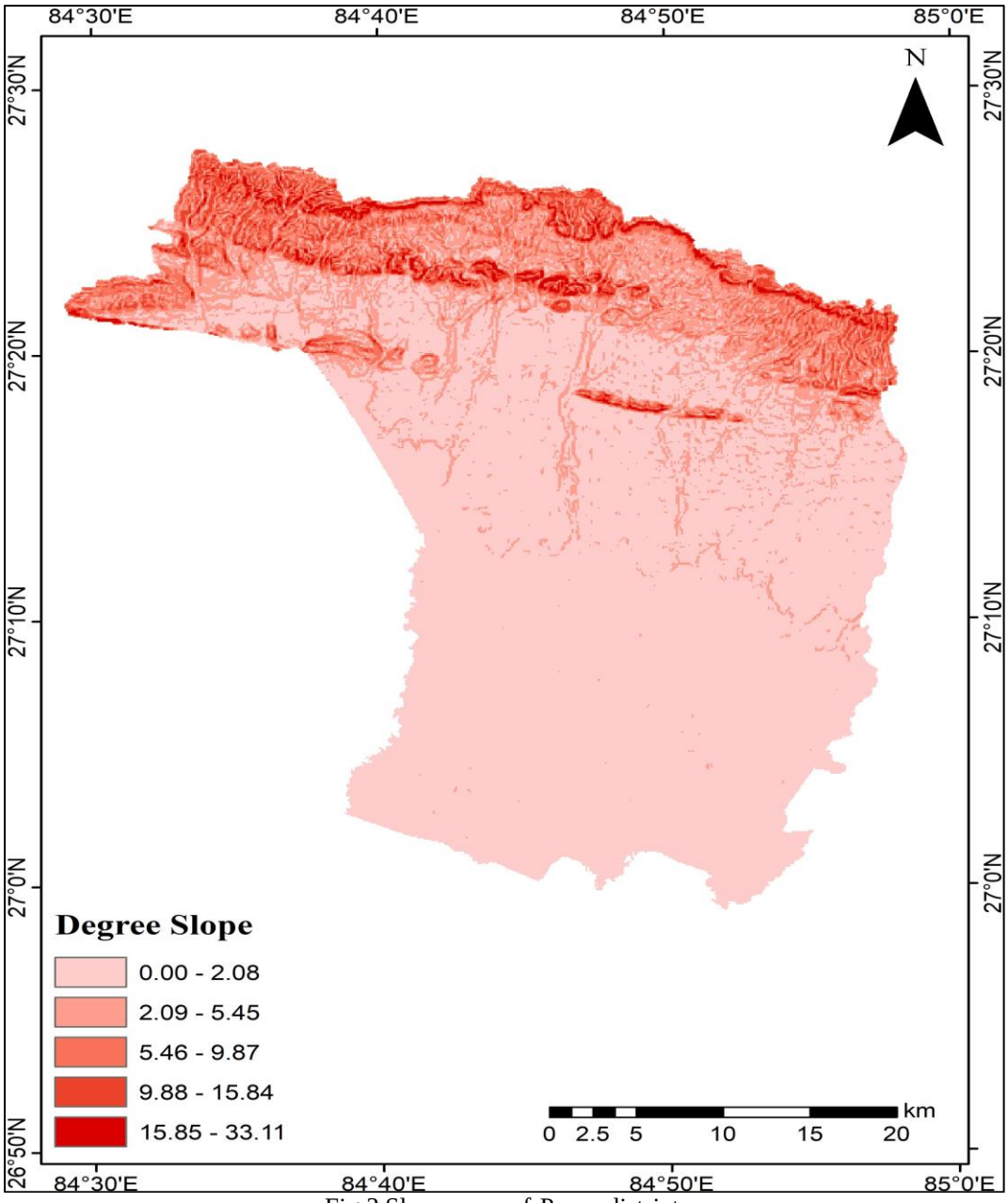

Fig 3 Slope map of Parsa district

ISSN No:-2456-2165 https://doi.org/10.38124/ijisrt/25mar287

Similarly, 14.99 % (202.88 km^2), 8.36 % (113.14 km^2), 4.62 % (62.54 km^2) and 1.49 % (20.13 km^2) of total land lies in the slope range of 2.08° to 5.45°, 5.45° to 9.87°, 9.87° to 15.84° and 15.84° to 33.11° respectively.

➢ *Geology*

Geology is a highly decisive parameter for groundwater recharge process as it controls the occurrence, movement, and storage of groundwater [3]. Similarly, physical make-up of rocks and sediments is defined by lithology and includes mineral composition, grain size and packing of grain [46]. Study area can be divided into different geological categories from north to south. Geological data was also obtained from regional database system of ICIMOD [37] which was used in the GIS environment. According, to the interpreted data, Parsa district is divided into five geological classes and geological map of Parsa district is presented in Figure 4.

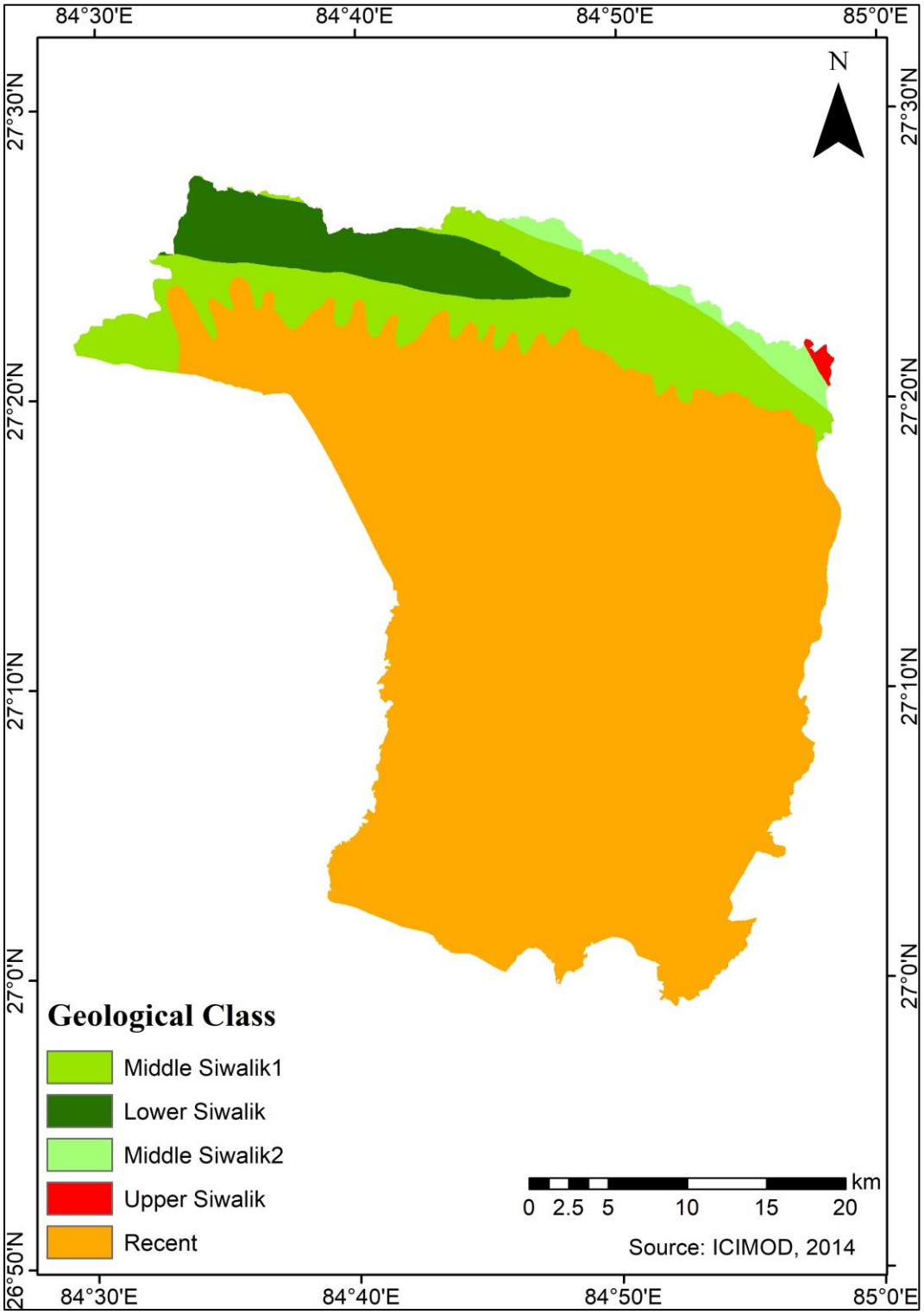

Fig 4 Geological Map of Parsa District

ISSN No:-2456-2165 https://doi.org/10.38124/ijisrt/25mar287

Each geological category has different physical rock characteristics which controls the percolation and infiltration of water flow and affects the groundwater recharge [38, 9]. Nature of rocks at the outcrops along with topography, slope and nature of soils are some of the factors through which geology controls recharge [46].

Upper Siwalik covers 0.17 % (2.24 km^2) of total land, 12.74 % (172.40 km^2) belong to Middle Siwalik1 and 1.58 % (21.44 km^2) was covered by Middle Siwalik2. Similarly, 6.08 % (82.25 km^2) was covered by Lower Siwalik and majority of the land i.e. 79.43 % (1074.66 km^2) was covered by Recent.

➢ *Drainage Density*

Drainage density is the ratio of total drainage length to total basin area and is expressed in km/km^2. Drainage density is an important parameter for determining groundwater potential zones as it is greatly related to permeability and infiltration capacity [9].

The assessment of the characteristics of the groundwater recharge zone is done by the help of structural analysis of a drainage network [38]. Along the major drainage channels, we can discover very good and good zonal categories [17]. Drainage density value can act as basis of categorization when developing a groundwater potential map. Areas with high drainage densities indicate low permeability, hence low groundwater potential and vice versa [6, 16, 9]. Closeness of the spacing of the stream channels is defined by drainage density [42]. Study area with low to moderate drainage density values indicate less river channel/drainage length. Areas with higher drainage density values indicate abundant river channels/drainage network.

For drainage density, data of the major river types of Nepal was obtained from DoS. Major river types of Parsa district were clipped from the main data in GIS environment and after that drainage density value was calculated. Calculation revealed that the drainage density of Parsa district lies in the range of 0.00 km/km^2 to 4.12 km/km^2 provided in Figure 5 with 34.90 % (472.26 km^2) of total land lying in the range of 0.00 km/km^2 to 1.00 km/km^2.

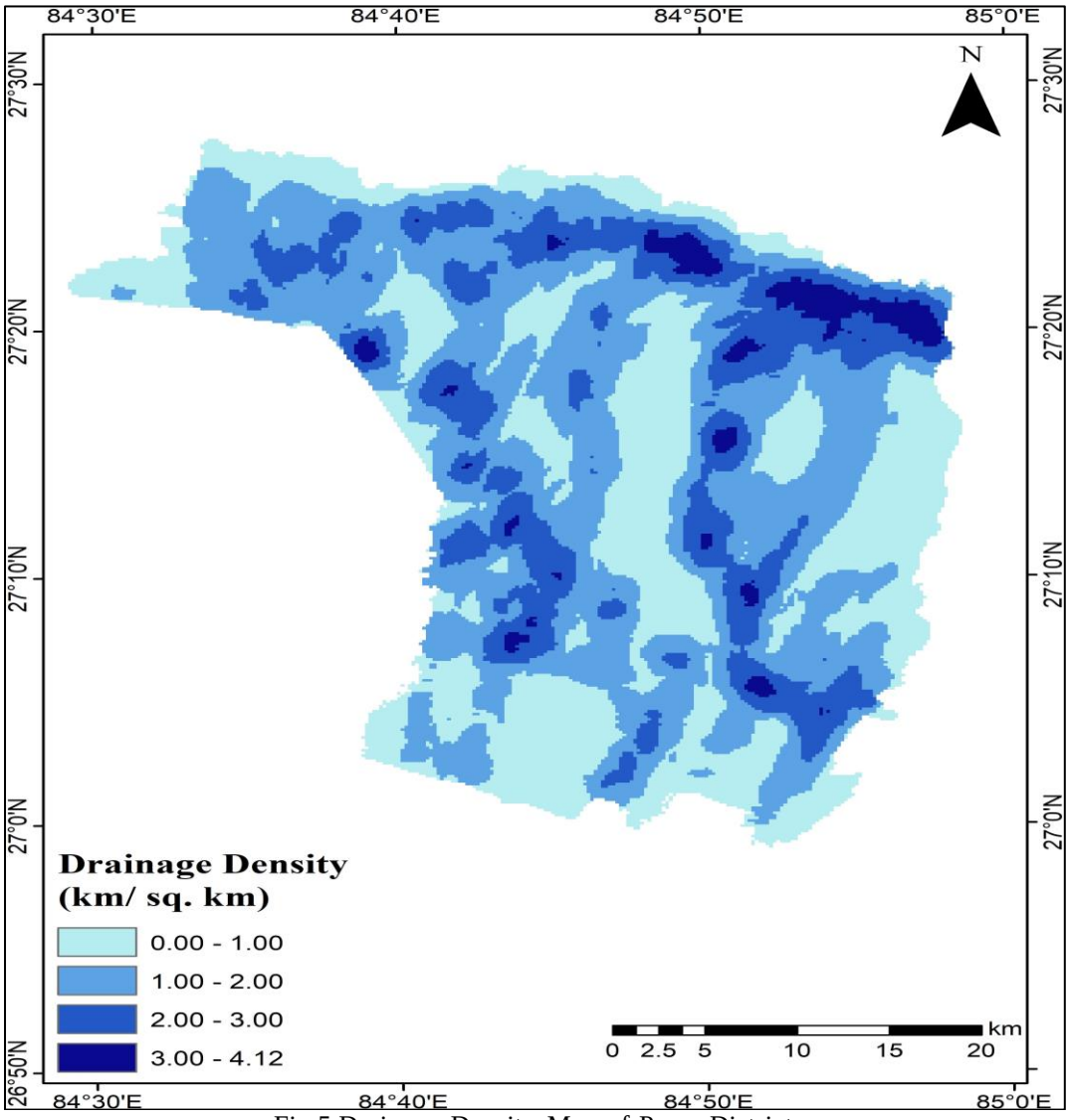

Fig 5 Drainage Density Map of Parsa District

ISSN No:-2456-2165 https://doi.org/10.38124/ijisrt/25mar287

Similarly, 43.63 % (590.27 km^2), 18.37 % (248.60 km^2), and 3.09 % (41.87 km^2) of total land lies in the drainage density range of 1.00 km/km^2 to 2.00 km/km^2, 2.00 km/km^2 to 3.00 km/km^2, and 3.00 km/km^2 to 4.12 km/km^2 respectively.

➢ *Precipitation*

Hydrological cycle and groundwater recharge is controlled by precipitation [42, 9]. Rainfall is a lifeline in the tropical and sub-tropical regions as it is the major source of groundwater recharge [38]. The precipitation characteristics should be determined to outline the groundwater potential of an area. The infiltration rate of runoff water is directly dependent on rainfall distribution along with the slope gradient; hence the possibility of groundwater potential zones also increases in areas with high rainfall [45]. Multiple years of data (say 30 years) of nearby stations of study area can be used to calculate the precipitation distribution according to the ordinary Kriging interpolation method and its application are common for groundwater level interpolation [47].

Precipitation data from 1990-2021 recorded by four different climatic stations was collected from DHM [32]. Collected data was interpreted in GIS environment and precipitation map provided in Figure 6 was developed with 5.54 % (74.91 km^2) of area lying in the precipitation range of 1555.20 mm to 1678.84 mm.

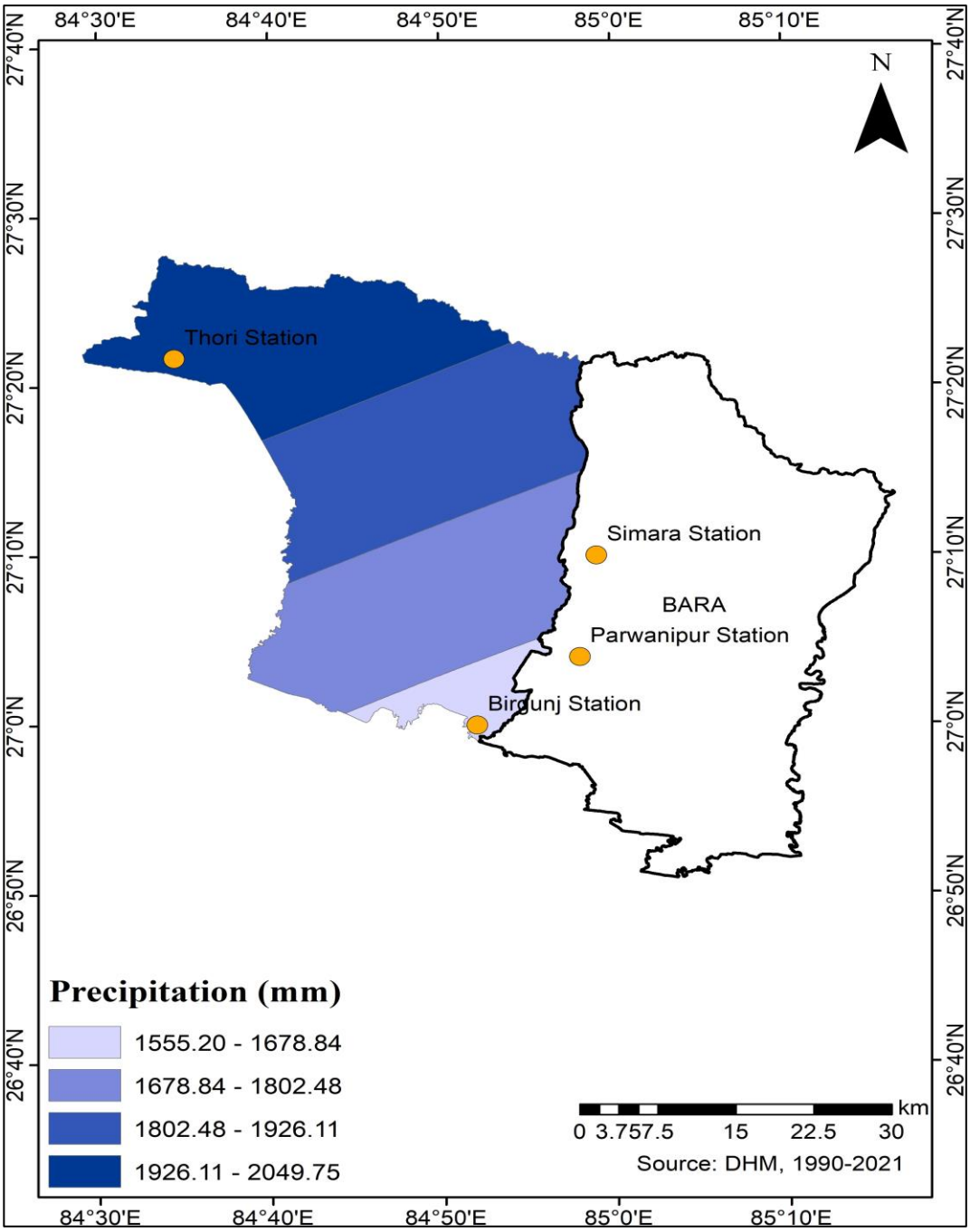

Fig 6 Precipitation Map of Parsa District

ISSN No:-2456-2165 https://doi.org/10.38124/ijisrt/25mar287

Similarly, 32.31 % (437.17 km^2), 32.66 % (441.91 km^2), and 29.49 % (399.02 km^2) of total land lies in the precipitation range of 1678.84 mm to 1802.48 mm, 1802.48 mm to 1926.11 mm, and 1926.11 mm to 2049.75 mm respectively.

➢ *Lineament Density*

Linear units linked with geological and geomorphological processes are defined by lineaments. Structural features namely fractures or faults or joints and surficial expressions of underlying geology are indicated by lineaments [46]. Tectonic deformation zones, interfluves, valleys, and ridgelines, etc. can be represented by lineaments [48, 9]. Lineaments are significant hydrogeological entity as they act as conduits for the flow of groundwater and the favourable zonal categories are along major lineaments [17]. Movement of groundwater is affected by lineaments as they represent weakness zones and increase the possibility of infiltrations to the groundwater. Lineament density is defined as the total length of all lineaments divided by considered area and is expressed in km/km^2. High lineament density indicates that the area is favourable for groundwater potential zones [45]. Groundwater potential increases with increase in lineament density value. Hence, lineament density and groundwater potential have directly proportional relationship.

For lineament density, help of Digital Elevation Model (DEM) data was taken from which hill shade was derived in GIS. Lineament density value was calculated by manually drawing lineaments in GIS with four different combinations of azimuth and altitude. Calculation revealed that the lineament density of Parsa district lies in the range of 0.00 km/km^2 to 0.77 km/km^2 provided in Figure 7 with 81.76 % (1106.27 km^2) of total land lying in the range of 0.00 km/km^2 to 0.08 km/km^2.

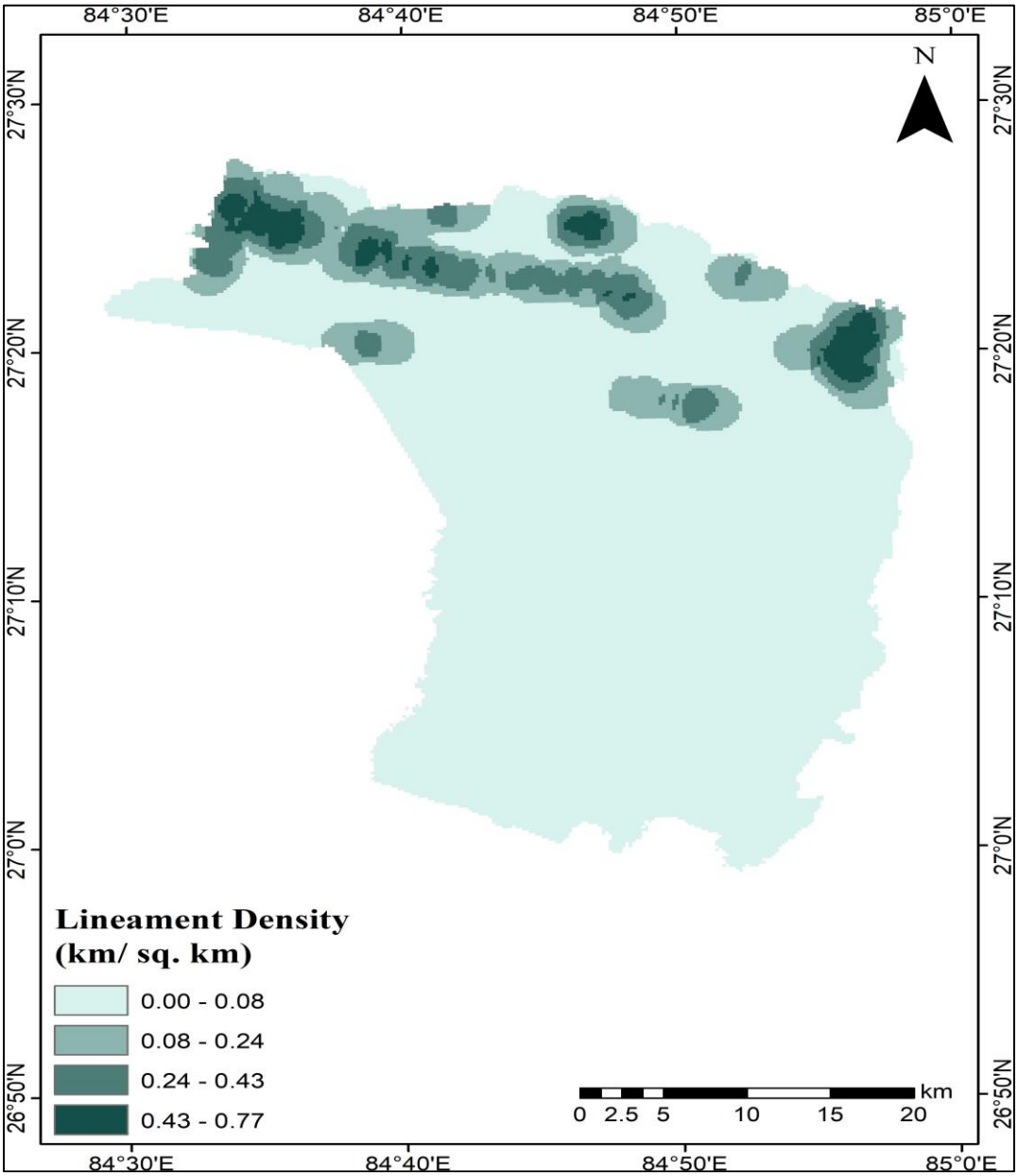

Fig 7 Lineament Density Map of Parsa District

ISSN No:-2456-2165 https://doi.org/10.38124/ijisrt/25mar287

In the same way, 10.08 % (136.43 km^2), 5.83 % (78.86 km^2), and 2.32 % (31.44 km^2) of total land lies in the lineament density range of 0.08 km/km^2 to 0.24 km/km^2, 0.24 km/km^2 to 0.43 km/km^2, and 0.43 km/km^2 to 0.77 km/km^2 respectively.

➢ *Soil*

Soil is a vital factor for depicting groundwater potential zones [45]. Soil properties such as structure, porosity, adhesion and consistency directly relate to the physical conditions of soil [6]. Influence of shallow groundwater may be significant on the components of water balance based on climate, soil texture and depth to water table [49]. The rate of infiltration in an area is controlled by soil texture [3]. Normally, thick alluvial soils adversely affect recharge that leads to high retention storage during the rainy season and eventually vegetation extracts water present in the soil in the following dry season [41]. Shallow tubewells can be constructed in areas that have medium to coarse sand with gravel [30]. Areas of highest permeability are characterized with free silty-clay matrix layers and such matrix layers are the most appropriate for artificial recharge of aquifer [50].

In Terai of Nepal, soil type such as dystric cambisols and eutric fluvisols may be available [51]. Dystric cambisols are infertile acid brown forest soils or acid brown wooded soils with changes in colour, structure and consistencies that results from weathering in-situ. Eutric fluvisols is fertile soil type of floodplains and alluvial deposits. Eutric fluvisols soil type may also occur in areas that may predominantly have dystric cambisols.

Soil data of Nepal was obtained from database of FAO [36] and data of Parsa district was clipped in the GIS environment. The calculation showed that the major soil type was eutric fluvisols and dystric cambisols which are presented in Figure 8.

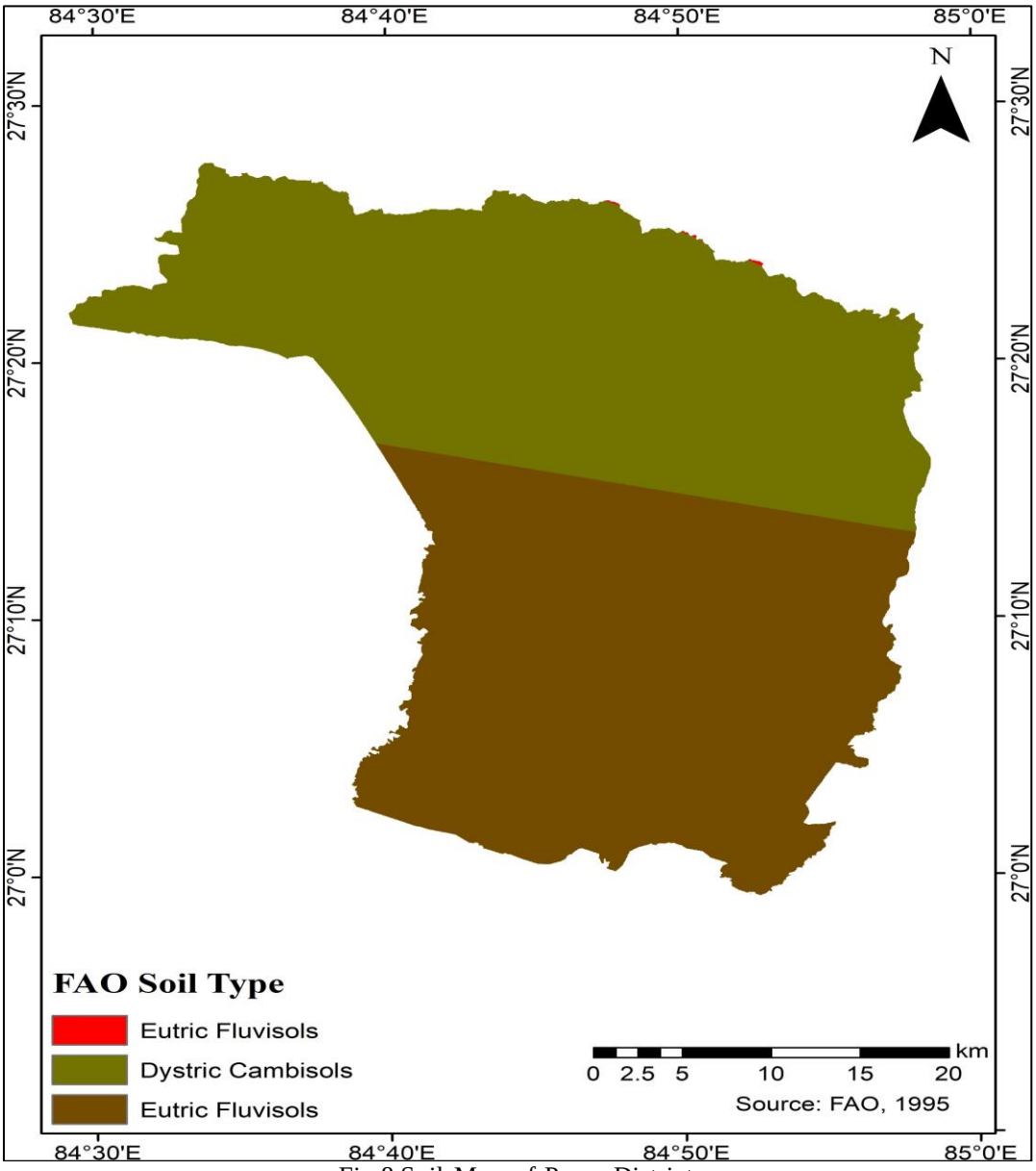

Fig 8 Soil Map of Parsa District

ISSN No:-2456-2165 https://doi.org/10.38124/ijisrt/25mar287

Dystric cambisols was found in 50.17 % (678.81 km^2) of total area while eutric fluvisols in northern part covered 0.02 % (0.32 km^2) area and 49.81 % (673.87 km^2) of total area in southern part of the district.

B. Applying AHP

GIS along with AHP was used to create an overlay map with thematic layers that includes land cover, slope, geology, drainage density, precipitation, lineament density and soil type which are presented in Figure 2, Figure 3, Figure 4, Figure 5, Figure 6, Figure 7 and Figure 8 respectively. Overlay was done in GIS using the weighted overlay tool. Application of AHP was done in four steps that included (1) appropriate weights assigned to the themes based on expert opinions and literature reviews, (2) pairwise comparison between thematic layers, (3) calculation of weights of parameters, and (4) estimation of Consistency Ratio (CR). Assigned weights of the seven influencing theme along with the basis of categorization is presented in Table 2 while Table 3 presents pairwise comparison between corresponding thematic layers and calculation of geometric mean (GM) along with the calculation of normalized weight.

Table 2 Weight Assignment Criteria of Thematic Maps of Study Area

Themes	Basis of Categorization	Assigned Weight
Land cover (LC)	Land cover type	7.0
Slope (S)	Slope degree	5.0
Geology (G)	Landform type	4.5
Drainage density (DD)	Drainage density value	4.0
Precipitation (P)	Precipitation value	3.5
Lineament density (LD)	Lineament density value	3.0
Soil type (ST)	Soil type	2.5

Table 3 Pairwise Comparison between Thematic Layers of Study Area

	LC	S	G	DD	P	LD	ST	GM	Normalized Weight
LC	7/7	7/5	7/4.5	7/4	7/3.5	7/3	7/2.5	1.75	0.24
S	5/7	5/5	5/4.5	5/4	5/3.5	5/3	5/2.5	1.25	0.17
G	4.5/7	4.5/5	4.5/4.5	4/5/4	4.5/3.5	4.5/3	4.5/2.5	1.12	0.15
DD	4/7	4/5	4/4.5	4/4	4/3.5	4/3	4/2.5	1.00	0.14
P	3.5/7	3.5/5	3.5/4.5	3.5/4	3.5/3.5	3.5/3	3.5/2.5	0.87	0.12
LD	3/7	3/5	3/4.5	3/4	3/3.5	3/3	3/2.5	0.75	0.10
ST	2.5/7	2.5/5	2.5/4.5	2.5/4	2.5/3.5	2.5/3	2.5/2.5	0.62	0.08
Total								7.36	1.00

Similarly, the themes were categorized into sub-classes and the ranks were also assigned to those sub-classes. Assigned ranks of sub-classes of themes are presented in Table 4. After entering the information presented in Table 4 in the weighted overlay tool in GIS, an overlay map with a new theme was produced that represented the groundwater potential zones.

Consistency ratio of pairwise comparison was calculated using Equation 2 given by Saaty, 1980.

$$CR = \frac{CI}{RI} \quad (2)$$

Where CR is consistency ratio, CI is consistency index and RI is random consistency index whose value is dependent on the number of parameters that have been compared. Consistency index can be calculated by Equation 3 provided by Saaty, 1980 [20].

$$CI = \frac{\lambda - n}{n-1} \quad (3)$$

Where n is the number of parameters that were used and λ is the average eigen value of the consistency vectors. The RI value depends upon the number of parameters being compared. As per Saaty, 1980 [20] the RI value for 'n = 7' is 1.32 and the details are provided in Table 5. The calculated CR should be 0.10 or less to be acceptable. Therefore, if the CR is greater than 0.10, assigned weights are not consistent and the pairwise matrix should be reconstructed.

λ calculated as = 7.0362, and CI = 7.0362–7/7-1 = 0.0060. CR = 0.0060/ 1.32 = 0.0046. Therefore, the consistency ratio is calculated as 0.0046. Since 0.0046 < 0.10, weights assigned to the parameters are accepted and exhibit trustworthy values because they are very close to the perfect consistency value i.e. 0.

Table 4 Values of Random Consistency Index (RI)

Number of Parameters (n)	RI	Number of Parameters (n)	RI	Number of Parameters (n)	RI
1	0.00	6	1.24	11	1.51
2	0.00	7	1.32	12	1.48
3	0.58	8	1.41	13	1.56
4	0.90	9	1.45	14	1.57

ISSN No:-2456-2165 https://doi.org/10.38124/ijisrt/25mar287

5	1.12	10	1.49	15	1.59

Table 5 Assigned Ranks of Sub-Classes of Themes

Weight (%)	Themes	Sub-Classes	Area (km^2)	Assigned Rank
24	Land cover	Forest	762.56	7
		Shrubland	23.37	7
		Flooded vegetation	0.00*	8
		Agriculture area	473.41	8
		Barren area	11.99	6
		Water body	4.75	5
		Built-up area	76.92	1
17	Slope (°)	0.00-2.08	954.31	8
		2.08-5.45	202.88	7
		5.45-9.87	113.14	5
		9.87-15.84	62.54	3
		15.84-33.11	20.13	1
15	Geology	Upper Siwalik	2.24	1
		Middle Siwalik1	172.40	2
		Middle Siwalik2	21.44	3
		Lower Siwalik	82.25	5
		Recent	1074.66	7
14	Drainage density (km/km^2)	0.00-1.00	472.26	7
		1.00-2.00	590.27	5
		2.00-3.00	248.60	3
		3.00-4.12	41.87	1
12	Precipitation (mm)	1555.20-1678.84	74.91	5
		1678.84-1802.48	437.17	6
		1802.48-1926.11	441.91	7
		1926.11-2049.75	399.02	8
10	Lineament density (km/km^2)	0.00-0.08	1106.27	1
		0.08-0.24	136.43	3
		0.24-0.43	78.86	5
		0.43-0.77	31.44	7
08	Soil type	Eutric fluvisols	0.32	7
	16	Dystric cambisols	678.81	6
		Eutric fluvisols	673.87	7

* Area of flooded vegetation is 685.22 m^2

C. Determination of Groundwater Potential Zones

For determination of groundwater potential zones, Groundwater Potential Index (GWPI) [23, 46, 9] have been used as presented in Equation 4:

$$\sum_{w=1}^{m}\sum_{j=1}^{n}(Wj * Xi) \quad (4)$$

Where m is the total number of parameters, n is the total number of subclasses of a parameter, W_j is the normalized weight of the jth parameter, and X_i is the normalized rank of the subclasses of parameters. The calculation was conducted, and groundwater potential zones were determined that is presented in Figure 9. Final values were classified in 4 classes as poor, moderate, good, and very good. Results revealed that an area of about 1.09 % (14.67 km^2), 15.76 % (213.26 km^2), 62.15 % (840.90 km^2) and 21.00 % (284.18 km^2) of study area exhibited poor, moderate, good, and very good groundwater potential zone respectively. Mainly in the north-eastern part of the district, the groundwater potential was found to be poor although the area lies within the National Park. This is because that section of the district lay in the region that was steeper and had higher drainage density value along with the presence of dystric cambisols soil which is less fertile than eutric fluvisols. So, the chance of infiltration becomes less with the above-mentioned conditions.

ISSN No:-2456-2165 https://doi.org/10.38124/ijisrt/25mar287

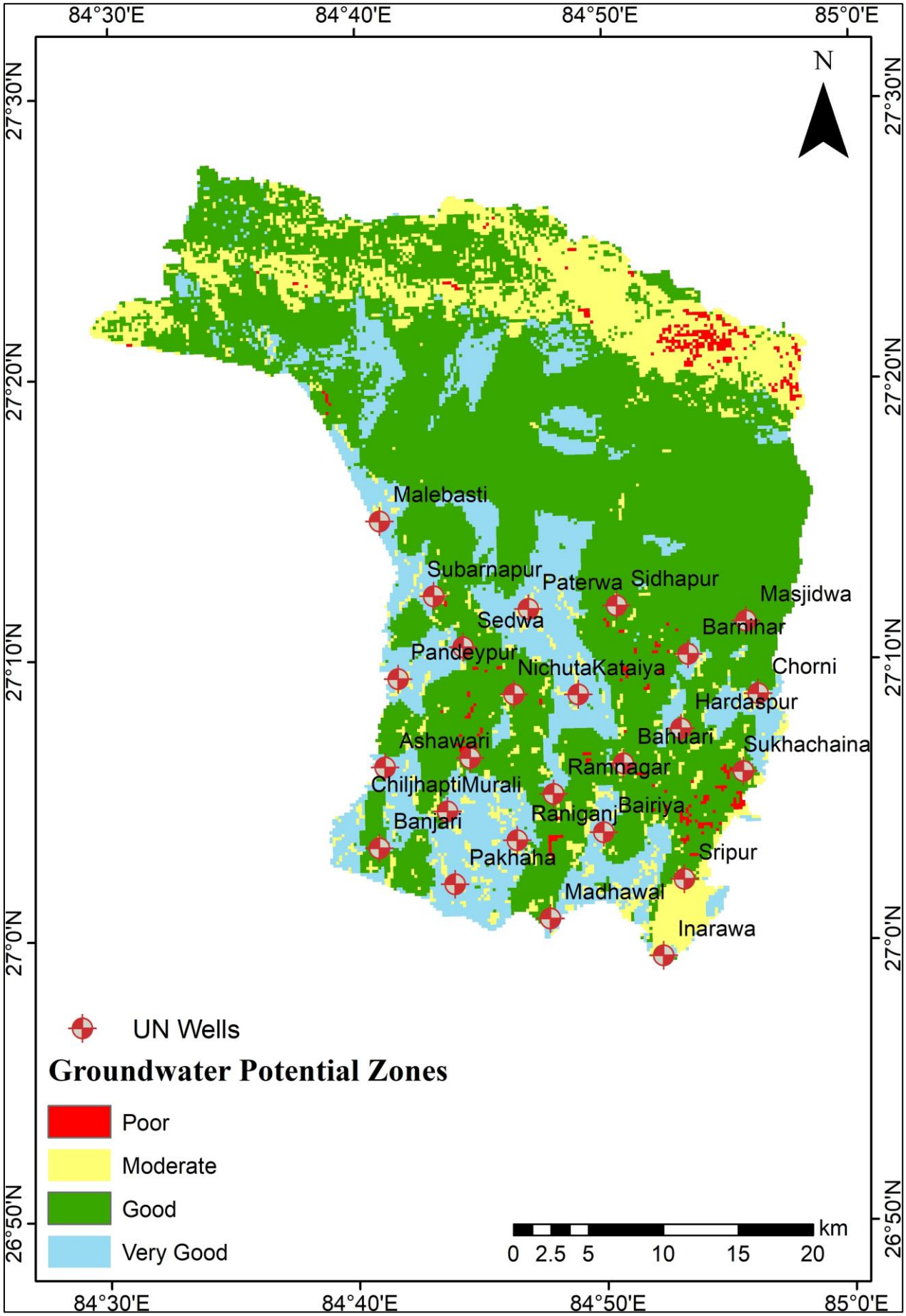

Fig 9 Groundwater Potential Zones Map of Parsa District

ISSN No:-2456-2165 https://doi.org/10.38124/ijisrt/25mar287

D. Validation of Results

For validation of groundwater potential zone, 25 UN wells were also added as layer in the new overlay thematic map within GIS environment. These 25 wells were chosen because the report of UNDP and HMG 1990 had specified the pumping test of newly drilled 25 UN shallow wells in 1990. These 25 UN wells were also dug with the aim of replacing the nearby dug wells and private shallow tubewells [30]. This showed that 13 wells were in very good groundwater potential zone, 10 wells were in good groundwater potential zone and 2 wells namely in Inarawa and Bahuari were present in moderate groundwater potential zone. Hence distribution of wells verified the results.

E. Water Storage Potential of Shallow Aquifer by Permeable Layer

For the calculation of permeable layer, 48 wells were considered that were based upon the report of UNDP and HMG 1990 [30]. For this case 25 UN wells and 23 wells drilled by Japanese Red-Cross Society were considered. Not all the wells were pump tested, but all had lithological data. From the well logs, the depth of permeable layer was possible to calculate. Therefore, these 48 wells were considered to improve the data representation. Sand and gravel were only considered as permeable layer whereas clay as excluded as permeable layers. Sand layer included only sand and sand coarse with gravel. Similarly, gravel layer included only gravel and gravel with sand. When the depth up to 50 m for 48 wells were considered, the total permeable depth (sand and gravel layer) was out to be 493.00 m. Out of total depth of permeable layer, sand has a depth of 286.60 m and gravel is 23.60 m deep. In the same way, sand coarse with gravel is 52.10 m deep whereas gravels with sand have a depth of 130.70 m. The distribution of thickness of permeable layers within the depth of 50 m in Parsa district is presented in Figure 10.

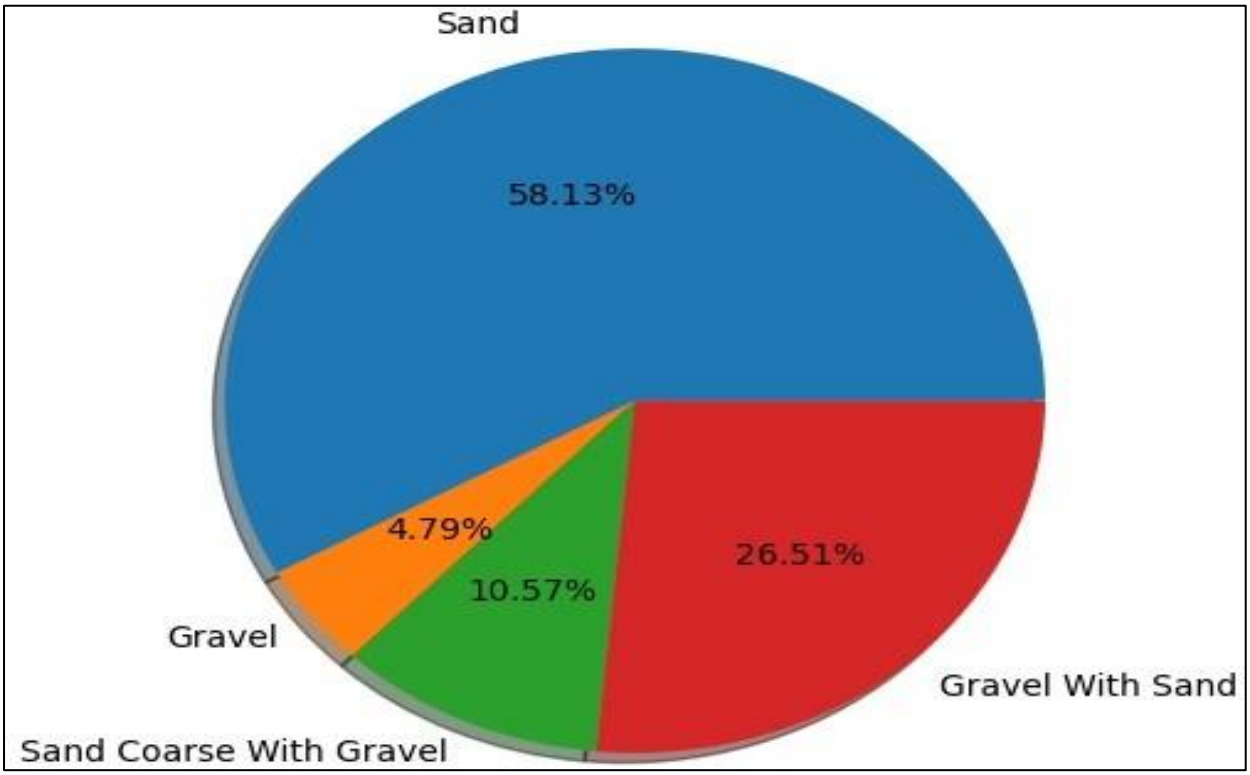

Fig 10 Distribution of Thickness of Permeable Layer within the Depth of 50 m

For sand coarse with gravel, the assumption was that it had depth of 60 % sand and 40 % gravel. Similarly, for gravel with sand, the assumption was that it had depth of 60 % gravel and 40 % sand. This resulted in overall depth of sand as 370.14 m (75.08 %) and depths of gravel as 122.86 m (24.92 %). The range of permeable layer within the depth of 50 m is also presented in Figure 11 in which the depth of permeable layer for all 48 wells was interpolated by ordinary Kriging method within the GIS environment. Also, the area covered by these ranges was also calculated in ArcGIS.

Depth of permeable layer having range of 9.21 m to 10.50 m had an area of 499.29 km^2 whereas depth range of 10.50 m to 11.79 m had an area of 443.69 km^2.

ISSN No:-2456-2165 https://doi.org/10.38124/ijisrt/25mar287

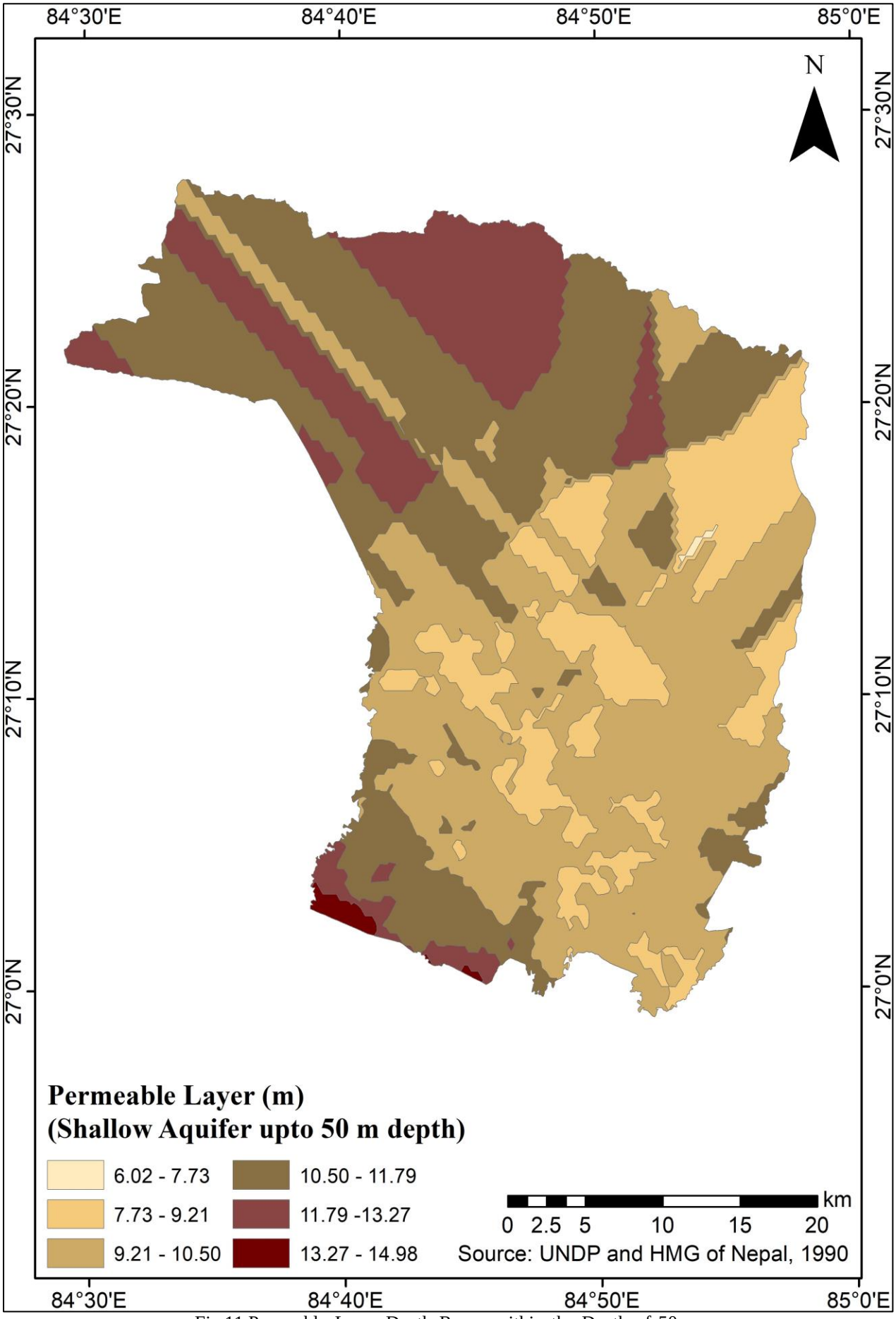

Fig 11 Permeable Layer Depth Range within the Depth of 50 m

ISSN No:-2456-2165 https://doi.org/10.38124/ijisrt/25mar287

Similarly, depth of permeable layer having range of 6.02 m to 7.73 m, 7.73 m to 9.21 m, 11.79 m to 13.27 m, and 13.27 m to 14.98 m covered an area of 1.08 km^2, 201.64 km^2, 201.10 km^2 and 6.21 km^2 respectively.

Based on Freeze and Cherry, 1979 [29]; sand porosity was assumed as 37 % and gravel porosity was assumed as 32 %. By multiplying the mid-value depth of permeable layer with sand distribution (i.e. 75.08 %) and gravel distribution (i.e. 24.92 %), we obtained the depth of sand and depth of gravel provided in Table 6. These depths were again multiplied with above mentioned respective porosities and ultimately with the area covered by depth of permeable range to obtain the water storage potential in permeable layer of shallow aquifer up to depth 50 m. The calculation of water storage potential in permeable layer is presented in Table 7.

Table 6 Calculation of Sand and Gravel Depth

Mid-Value of Permeable Layer (m)	Permeable Layer of Sand (%)	Sand Depth (m)	Permeable Layer of Gravel (%)	Gravel Depth (m)
6.87	75.08	5.16	24.92	1.71
8.47	75.08	6.36	24.92	2.11
9.86	75.08	7.40	24.92	2.46
11.14	75.08	8.37	24.92	2.78
12.53	75.08	9.41	24.92	3.12
14.13	75.08	8.61	24.92	3.52

Table 7 Water storage potential in permeable layer up to depth 50 m

Sand Depth (m)	Sand Porosity (%)	Gravel Depth (m)	Gravel Porosity (%)	Area (km^2)	Water Storage Potential (MCM)
5.16	37.00	1.71	32.00	1.08	2.65
6.36	37.00	2.11	32.00	201.64	610.52
7.40	37.00	2.46	32.00	499.29	1759.27
8.37	37.00	2.78	32.00	443.69	1767.99
9.41	37.00	3.12	32.00	201.10	901.03
8.61	37.00	3.52	32.00	6.21	31.38
					Total: 5072.84

Hence, from the calculation presented in Table 6 and Table 7, a total of 5072.84 MCM of water can be stored in the permeable layer of shallow aquifer that has a depth up to 50 m within Parsa district. Also, as the depth of the well increases, greater yield in the Terai and inner Terai regions of Nepal can be expected [52].

Similar study conducted in Dun valley aquifers in Chitwan, inner Terai region of Nepal, had estimated a total groundwater storage of 87.31 MCM per year for a recharge area of 70.8 km^2 [53].

Based on the results, the stakeholders of the region will be able to investigate the problem of water availability with some figures. As we know, the population is increasing and the demand for water is also increasing, especially the groundwater in all parts of the world. The rising demand for water in Terai is also supported by the fact that more than half of the population of Nepal resides in the Terai. The flatlands of Terai have fertile soil which favours agricultural activities, and the most common source of water used is the groundwater. The GIS and AHP method used in this study will not only save time but also, the economic resources of a developing country such as Nepal. This integration of GIS and AHP can be used before conducting hydrogeological explorations and the themes used in this paper can be used for all the flatlands of the region. Moreover, pumps for irrigation, handpumps or tubewells could be installed by the local government based on the groundwater potential zone map and the availability of the water in that zone could be anticipated with the help of the thickness of the aquifer. Not knowing the volume of groundwater to be supplied from an aquifer based on the demand could be balanced based on the opinions of hydrogeologists, engineers, economists, and environmental lawyers. This will not only reduce the unplanned exploitation of groundwater resources but also allows the replenishment of the aquifer.

V. CONCLUSION

The aim of the paper was to determine the groundwater potential zones and storage capacities of shallow aquifer in Parsa district. Groundwater potential zones in Parsa district was evaluated using GIS and AHP. An area of about 1.09 % (14.67 km^2), 15.76 % (213.26 km^2), 62.15 % (840.90 km^2) and 21.00 % (284.18 km^2) of study realm exhibited poor, moderate, good, and very good groundwater potential zone respectively. Results suggest that most of the very good groundwater potential zones lie below the southern boundary of National Parks. Areas under poor groundwater potential zone requires adept planning and management for protection of groundwater resources [54]. The results from this study can be used as guidelines for planning upcoming artificial recharge projects in the study area [45]. GIS-AHP method can be applied to whole Terai belt for the investigation of appropriate areas.

ISSN No:-2456-2165 https://doi.org/10.38124/ijisrt/25mar287

Based on lithological data of 48 wells, approximately 70 % of total study area has depth of permeable layer in between 9.21 m to 11.79 m within depth of 50 m of shallow aquifers as obtained by ordinary Kriging method. Similarly, a total of 5072.84 MCM of water can be stored in the permeable layer (i.e. sand and gravel) of shallow aquifer that has a depth up to 50 m within Parsa district.

The limitation of AHP technique is the weight assignment which depends upon the perceptions of expert. GIS techniques can be effective for larger areas in identifying potential areas where detailed hydro-geological surveys for groundwater exploration can be done [55]. For future research, depth of permeable layer, recharge rate, groundwater depth and elevation could also be added as the parameter or theme. Also, the new hydrogeological surveys could provide new perspective regarding the aquifer thickness and the potential storage capacity. Hydrogeological survey in Parsa district post the 2015 earthquake of Nepal has not been conducted that could have certainly altered the aquifer characteristics.

ACKNOWLEDGEMENTS

The authors would like to thank Groundwater Resources Development Board, Babarmahal, Kathmandu for providing lithological data of 48 different wells present in Parsa district.

- Groundwater potential zone mapping using integrated GIS-AHP approach
- Seven environmental themes/parameters were used for mapping groundwater potential zones
- Based on lithology of 48 wells in Parsa district, potential storage capacity was calculated
- 25 UN shallow tube wells present in Parsa district validated the result

REFERENCES

[1]. S. Arunbose, Y. Srinivas, S. Rajkumar, N. C. Nair, S. Kaliraj, Remote sensing, GIS and AHP techniques based investigation of groundwater potential zones in the Karumeniyar river basin, Tamil Nadu, southern India, Groundwater for Sustainable Development 14 (2021) 100586.

[2]. S. R. Shrestha, G. N. Tripathi, D. Laudari, Groundwater resources of Nepal: An overview, Groundwater of South Asia (2018) 169–193.

[3]. A. Achu, J. Thomas, R. Reghunath, Multi-criteria decision analysis for delineation of groundwater potential zones in a tropical river basin using remote sensing, GIS and analytical hierarchy process (AHP), Groundwater for Sustainable Development 10 (2020) 100365.

[4]. L. F. Konikow, E. Kendy, Groundwater depletion: A global problem, Hydrogeology Journal 13 (1) (2005) 317–320.

[5]. P. Döll, H. Hoffmann-Dobrev, F. T. Portmann, S. Siebert, A. Eicker, M. Rodell, G. Strassberg, B. Scanlon, Impact of water withdrawals from groundwater and sur-face water on continental water storage variations, Journal of Geodynamics 59 (2012) 143–156.

[6]. S. Patra, P. Mishra, S. C. Mahapatra, Delineation of groundwater potential zone for sustainable development: A case study from Ganga alluvial plain covering Hooghly district of India using remote sensing, geographic information system and analytic hierarchy process, Journal of Cleaner Production 172 (2018) 2485–2502.

[7]. M. Shamsudduha, R. G. Taylor, K. M. Ahmed, A. Zahid, The impact of intensive groundwater abstraction on recharge to a shallow regional aquifer system: evidence from Bangladesh, Hydrogeology Journal 19 (4) (2011) 901–916.

[8]. C. Herbert, P. Döll, Global assessment of current and future groundwater stress with a focus on transboundary aquifers, Water Resources Research 55 (6) (2019) 4760– 4784.

[9]. T. Aykut, Determination of groundwater potential zones using geographical in-formation systems (GIS) and analytic hierarchy process (AHP) between Edirne-Kalkansogut (northwestern Turkey), Groundwater for Sustainable Development 12 (2021) 100545.

[10]. S. A. Mathias, H. S. Wheater, Groundwater Modelling in Arid and Semi-Arid Areas: An Introduction, Cambridge: Cambridge University Press, 2010.

[11]. M. Gad, M. El-Hattab, Integration of water pollution indices and drastic model for assessment of groundwater quality in El Fayoum depression, western desert, Egypt, Journal of African Earth Sciences 158 (2019) 103554.

[12]. D. Pathak, M. Gautam, Demarcation of groundwater prospect zones in lower reaches of Daraudi river basin, western Nepal, Journal of Environmental and Soil Sciences 4 (1) (2019) 440–447.

[13]. CBS, Preliminary Report of National Population Census 2021, Kathmandu: Central Bureau of Statistics (Retrieved 2022 from Central Bureau of Statistics, Kathmandu).

[14]. E. Sener, A. Davraz, M. Ozcelik, An integration of GIS and remote sensing in groundwater investigations: a case study in Burdur, Turkey, Hydrogeology Journal 13 (5) (2005) 826–834.

[15]. J. Krishnamurthy, N. Venkatesa Kumar, V. Jayaraman, M. Manivel, An approach to demarcate ground water potential zones through remote sensing and a geographical information system, International journal of Remote sensing 17 (10) (1996) 1867–1884.

[16]. D. Pinto, S. Shrestha, M. S. Babel, S. Ninsawat, Delineation of groundwater potential zones in the Comoro watershed, Timor Leste using GIS, remote sensing and analytic hierarchy process (AHP) technique, Applied Water Science 7 (1)

ISSN No:-2456-2165 https://doi.org/10.38124/ijisrt/25mar287

(2017) 503–519.
[17]. S. Solomon, F. Quiel, Groundwater study using remote sensing and geographic in-formation systems (GIS) in the central highlands of Eritrea, Hydrogeology Journal 14 (6) (2006) 1029–1041.
[18]. M. Gad, M. El Hattab, S. Galal, Assessment of the miocene aquifer in Wadi El Farigh area by using GIS techniques, NRIAG Journal of Astronomy and Geophysics 5 (2) (2016) 463–473.
[19]. P. Kulandaisamy, S. Karthikeyan, A. Chockalingam, Use of GIS-AHP tools for potable groundwater potential zone investigations—a case study in Vairavanpatti rural area, Tamil Nadu, India, Arabian Journal of Geosciences 13 (17) (2020) 1–15.
[20]. T. a Saaty, The analytic hierarchy process: Planning, priority setting, Resource Allocation (1980)
[21]. S. Roy, S. Hazra, A. Chanda, S. Das, Assessment of groundwater potential zones using multi-criteria decision-making technique: a micro-level case study from red and lateritic zone (RLZ) of West Bengal, India, Sustainable Water Resources Management 6 (1) (2020) 1–14.
[22]. J. Qadir, M. S. Bhat, A. Alam, I. Rashid, Mapping groundwater potential zones using remote sensing and GIS approach in Jammu Himalaya, Jammu and Kashmir, GeoJournal 85 (2) (2020) 487–504.
[23]. T. G. Andualem, G. G. Demeke, Groundwater potential assessment using GIS and re-mote sensing: A case study of Guna tana landscape, upper Blue Nile Basin, Ethiopia, Journal of Hydrology: Regional Studies 24 (2019) 100610.
[24]. S. D´ıaz-Alcaide, P. Mart´ınez-Santos, Advances in groundwater potential mapping, Hydrogeology Journal 27 (7) (2019) 2307–2324.
[25]. A. Chowdhury, M. Jha, V. Chowdary, B. Mal, Integrated remote sensing and GIS-based approaches for assessing groundwater potential in West Medinipur district, West Bengal, India, International Journal of Remote Sensing 30 (1) (2009) 231–250.
[26]. V. Ajay Kumar, N. Mondal, S. Ahmed, Identification of groundwater potential zones using RS, GIS and AHP techniques: A case study in a part of Deccan volcanic province (DVP), Maharashtra, India, Journal of the Indian Society of Remote Sensing 48 (3) (2020) 497–511.
[27]. T. Moodley, M. Seyam, T. Abunama, F. Bux, Delineation of groundwater potential zones in KwaZulu-Natal, South Africa using remote sensing, GIS and AHP, Journal of African Earth Sciences (2022) 104571.
[28]. M. Hasan, Y. Shang, G. Akhter, W. Jin, Evaluation of groundwater potential in Kabirwala area, Pakistan: A case study by using geophysical, geochemical and pump data, Geophysical Prospecting 66 (9) (2018) 1737–1750.
[29]. J. A. Cherry, R. A. Freeze, Groundwater, Englewood Cliffs, NJ: Prentice-Hall, 1979.
[30]. UNDP, HMG, Shallow groundwater investigations in Terai (Parsa district), NEP/86/025, Technical Report No. 23, Kathmandu: GWRDB (1990).
[31]. ESRI, Sentinel-2 land cover time series of the world from 2017-2021 (Retrieved June 15, 2022).
[32]. DHM, Monthly rainfall (1990-2021) of Parsa district (Retrieved February 15, 2022, from Department of Hydrology and Meteorology, Kathmandu).
[33]. USAID, NASA, ICIMOD, National Agricultural Drought Watch-Nepal, Kathmandu, Nepal: ICIMOD (Retrieved June 24, 2022, from http://tethys.icimod.org/apps/droughtnp/seasonal).
[34]. D. of Survey, Digital elevation model 100 m (Retrieved 2019).
[35]. D. of Survey, Rivers of Nepal (Retrieved 2019).
[36]. FAO, Digital Soil Map of the World, Rome: Land and Water Development Division, FAO (1995).
[37]. ICIMOD, Geology of Nepal, Kathmandu, Nepal: ICIMOD (2014).
[38]. H.-F. Yeh, C.-H. Lee, K.-C. Hsu, P.-H. Chang, GIS for the assessment of the groundwater recharge potential zone, Environmental geology 58 (1) (2009) 185–195.
[39]. K. Jinno, A. Tsutsumi, O. Alkaeed, S. Saita, R. Berndtsson, Effects of land-use change on groundwater recharge model parameters, Hydrological sciences journal 54 (2) (2009) 300–315.
[40]. D. N. Lerner, B. Harris, The relationship between land use and groundwater resources and quality, Land Use Policy 26 (2009) S265–S273.
[41]. J. J. De Vries, I. Simmers, Groundwater recharge: An overview of processes and challenges, Hydrogeology Journal 10 (1) (2002) 5–17.
[42]. P. Murmu, M. Kumar, D. Lal, I. Sonker, S. K. Singh, Delineation of ground-water potential zones using geospatial techniques and analytical hierarchy process in Dumka district, Jharkhand, India, Groundwater for Sustainable Development 9 (2019) 100239.
[43]. G. N. Delin, R. W. Healy, M. K. Landon, J. K. Böhlke, Effects of topography and soil properties on recharge at two sites in an agricultural Field 1, JAWRA Journal of the American Water Resources Association 36 (6) (2000) 1401–1416.
[44]. M. A. Rahman, B. Rusteberg, R. Gogu, J. L. Ferreira, M. Sauter, A new spatial multi-criteria decision support tool for site selection for implementation of managed aquifer recharge, Journal of environmental management 99 (2012) 61–75.
[45]. N. S. Magesh, N. Chandrasekar, J. P. Soundranayagam, Delineation of groundwater potential zones in Theni district, TamilNadu,

ISSN No:-2456-2165 https://doi.org/10.38124/ijisrt/25mar287

using remote sensing, GIS and MIF techniques, Geoscience frontiers 3 (2) (2012) 189–196.
[46]. G. B. Lentswe, L. Molwalefhe, Delineation of potential groundwater recharge zones using analytic hierarchy process-guided GIS in the semi-arid Motloutse watershed, eastern Botswana, Journal of Hydrology: Regional Studies 28 (2020) 100674.
[47]. T. Nayak, S. Gupta, R. Galkate, GIS based mapping of groundwater fluctuations in Bina basin, Aquatic Procedia 4 (2015) 1469–1476.
[48]. G. Jordán, B. Meijninger, D. Van Hinsbergen, J. Meulenkamp, P. Van Dijk, Ext-raction of morphotectonic features from DEMs: Development and applications for stu-dy areas in Hungary and NW Greece, International journal of applied earth observat-ion and geoinformation 7 (3) (2005) 163–182.
[49]. M. E. Soylu, R. L. Bras, Detecting shallow groundwater from spaceborne soil moisture observations, Water resources research 57 (2) (2021) e2020WR029102.
[50]. A. Sendrős, M. Himi, R. Lovera, L. Rivero, R. Garcia-Artigas, A. Urruela, A. Casas, Geophysical characterization of hydraulic properties around a managed aquifer recharge system over the Llobregat river alluvial aquifer (Barcelona Metropolitan Area), Water 12 (12) (2020) 3455.
[51]. F A O-UNESCO, Soil Map of the World (Vol.1), Paris: UNESCO (1974).
[52]. D. Pathak, Status of groundwater exploitation and investigation in Terai and inner Terai region of Nepal, Bulletin of Nepal Hydrogeological Association 3 (2018) 77–83.
[53]. R. Neupane, S. D. Shrestha, Hydrogeologic assessment and groundwater reserve evaluation in northwestern parts of Dun valley aquifers of Chitwan, inner Terai, Bulletin of the Department of Geology 12 (2009) 43–54.
[54]. S. R. Warghat, S. V. Kulkarni, S. Das, Groundwater potential zones identification using integrated remote sensing and GIS-AHP approach in semiarid region of Ma- harashtra, India, in: Case Studies in Geospatial Applications to Groundwater Re- sources, Elsevier, 2023, pp. 67–90.
[55]. H.-F. Yeh, Y.-S. Cheng, H.-I. Lin, C.-H. Lee, Mapping groundwater recharge potential zone using a GIS approach in Hualian River, Taiwan, Sustainable Environment Research 26 (1) (2016) 33–43.